Robust Fuzzy-Neural-Network Levitation Control Design for Linear Maglev Rail System with Nonnegative Inputs

Rong-Jong Wai[1], SENIOR MEMBER, IEEE, and Jeng-Dao Lee[2]
[1,2] Department of Electrical Engineering, Yuan Ze University, Chung Li 32026, Taiwan, R.O.C.
[1] e-mail: rjwai@saturn.yzu.edu.tw [2] e-mail: s929103@mail.yzu.edu.tw

***Abstract*—The levitation control in a linear magnetic-levitation (maglev) rail system is a subject of considerable scientific interest because of highly nonlinear behaviors. This study mainly designs a robust fuzzy-neural-network control (RFNNC) scheme for the levitated positioning of the linear maglev rail system with nonnegative inputs. In the model-free RFNNC system, an on-line learning ability is designed to cope with the problem of chattering phenomena caused by the sign action in backstepping control (BSC) design, and to ensure the stability of the controlled system without the requirement of auxiliary compensated controllers despite the existence of uncertainties. Moreover, the nonnegative outputs of the RFNNC system can be directly supplied to electromagnets in the maglev system without complicated control transformations for relaxing strict constrains in conventional model-based control methodologies. The effectiveness of the proposed control schemes for the levitation control of a maglev system is verified by numerical simulations, and the superiority of the RFNNC system is indicated in comparison with the BSC system.**

I. INTRODUCTION

Nowadays, magnetic levitation (maglev) techniques have been respected for eliminating friction due to mechanical contact, decreasing maintaining cost, and achieving high-precision positioning. Therefore, they are widely used in various fields, such as high-speed trains [1], [2], magnetic bearings [3], [4], vibration isolation systems [5], wind tunnel levitation [6] and photolithography steppers [7]. In general, maglev techniques can be classified into two categories: electrodynamic suspension (EDS) and electromagnetic suspension (EMS). EDS systems are commonly known as "repulsive levitation", and the corresponding levitation sources are from superconductivity magnets [8] or permanent magnets [9]. On the other hand, EMS systems are commonly known as "attractive levitation", and the magnetic levitation force is inherently unstable so that the control problem becomes more difficult. In this study, the EMS strategy is utilized for the fundamental levitation force of a linear maglev rail system, and the corresponding levitated positioning and stabilizing control of the maglev system is the major control objective to be manipulated via model-free control schemes.

The attractive levitation in the EMS system belongs to a nonnegative input system. Some researches focused on nonnegative input systems are addressed in [10], [11]. He and Luo [10] presented a new implementation method to achieve a constant switching frequency sliding-mode control. As designed, the equivalent control input was maintained at a nonnegative value between 0 and 1. Aracil *et al.* [11] introduced a method for obtaining stable and robust self-sustained oscillations in a class of single-input nonlinear systems of dimension $n \geq 2$ with a nonnegative input. Overall, partial mathematical models via complicated modeling processes or specific mechatronic device are usually required to design a suitable control law for achieving positioning demand. The aim of this study is to design a model-free control strategy for a maglev system to relax the extra requirement in model-based control design.

Nowadays, the concept of incorporating fuzzy logic into a neural network has grown into a popular research topic [12]. The integrated fuzzy neural-network system possesses the merits of both fuzzy systems [13] (e.g., humanlike IF-THEN rules thinking and ease of incorporating expert knowledge) and neural networks [14] (e.g., learning and optimization abilities, and connectionist structures). By this way, one can bring the low-level learning and computational power of neural networks into fuzzy systems and also high-level, humanlike IF-THEN rule thinking and reasoning of fuzzy systems into neural networks. Chakraborty and Pal [15] investigated a novel neuro-fuzzy system with simultaneous feature analysis and system identification in an integrated manner, and the system was designed by maintaining the nonnegative characteristic via positive learnable weights. However, the system stability is a latent problem to be challenged. Lin *et al.* [16] proposed a supervisory fuzzy-neural-network controller for periodic command tracking of a permanent magnet synchronous servo motor, where a supervisory controller was designed to stabilize the system states around a defined bound region. Though the stability of the control system was guaranteed, the auxiliary control design, constraint conditions and prior system information were required in the design process, e.g., the bound of the variation of system parameters and external load disturbance. Unfortunately, in many practical systems such bounds may not be available. Leu *et al*. [17] designed a robust adaptive fuzzy-neural controller for a straight-arm robot. The effect of all the unmodeled dynamics, modeling errors and external disturbances on the tracking error was attenuated by the error compensator, which was constructed by the fuzzy-neural inference; however, there still exist some constrained conditions in this complicated framework. The goal of this study is to design an intelligent control scheme with nonnegative outputs for the tracking and stabilizing control of a maglev system including actuator dynamics without the requirement of system information and constrained conditions, and the compensation of auxiliary control design.

1-4244-0136-4/06/$20.00 ©2006 IEEE

II. Dynamic Analysis of Maglev System

The entire framework of a linear maglev rail system is depicted in Fig. 1, which is a linear motion mechanism via electromagnetic suspension technique to reduce friction forces during linear movement for promoting the electric machinery efficiency and simplifying the mechanical design procedure. The bottom of this mechanism is a motion basal platform equipped with an I-shaped steel bridge as the rail body. By appropriately exciting the stator winding of a linear induction motor (LIM) fixed on the overhead I-shaped steel bridge, it will produce the thrust force to propel the moving platform in horizontal displacement, and the corresponding displacement can be measured by a linear encoder. Moreover, the fenders placed at the ends of the LIM are designed to avoid the problem of collision, and vertically auxiliary wheels are used to decrease friction forces before the moving platform has been suspended completely. In order to achieve the magnetic levitation object, four electromagnets under the bottom of the moving platform are adopted in this study. When the electromagnets are excited to attract the upper plate of the rail, the moving platform will be levitated, and the corresponding levitation height is acquired by a gap sensor. In addition, perpendicularly firm cubes are installed for holding the vertical angle between two conductor plates of the moving platform to reduce measure errors. When the transversal displacement is varied during linear movement, transversal auxiliary wheels are employed to guide the moving platform on the march. Under the description of the linear maglev rail system, it contains two sub-systems including propulsion and maglev systems. In the former, propulsion system could be considered as a LIM control problem in previous works [18]. Inherently unstable electromagnetic force and difficult attitude control of the moving platform is more interested to challenge in the latter. In this study, it focuses on the control problem of the maglev system without considering the thrust force and motion control of the LIM.

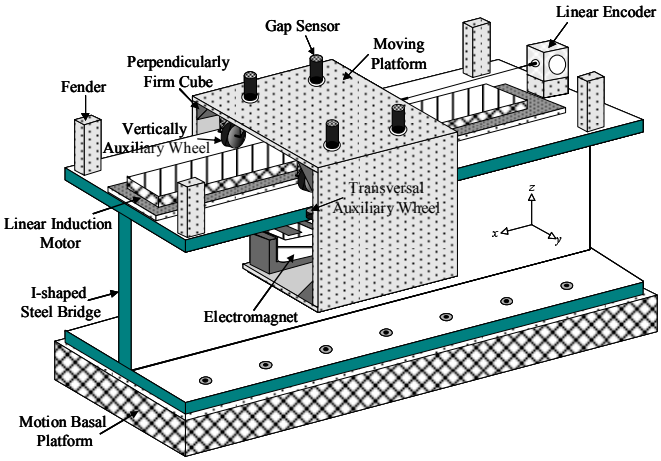

Fig. 1. Entire framework of linear maglev rail system.

In general, six degrees-of-freedom (DOF) could be considered in a fully suspended substance. According to Fig. 1, rotating along z-axis and moving in y-direction are constricted by transversal auxiliary wheels. Therefore, three kinds of motions including levitation (z, moving in z-direction), rolling (θ, rotating along x-axis) and pitching (ϕ, rotating along y-axis) should be considered to analyze the dynamic model of the maglev system. To regard the moving platform as a three-dimensional coordinate of the levitation stage, the sketch diagram of the maglev system is illustrated in Fig. 2, where l_t and w_t are the length and width of the moving platform. m_O, which is located at z-axis ($x=0$, $y=0$) in the three-dimensional coordinate, denotes the mass center of the moving platform. z_O and $z_{O,\max}$ are the central levitation height and its maximum limitation. By dividing the moving platform equally into four sub-platforms labeled as A, B, C and D areas, m_A, m_B, m_C, and m_D represent the mass centers of four sub-platforms, and the corresponding levitation heights labeled as z_A, z_B, z_C, and z_D are measured via gap sensors installed in the location of individual mass center. l_l and l_w are the horizontal distances from the mass centers of four sub-platforms to x-axis and y-axis, respectively. The applied control forces vector is represented as $\boldsymbol{f}=[f_A \quad f_B \quad f_C \quad f_D]^T$, in which f_A, f_B, f_C, and f_D of four sub-platforms are acquired through levitation forces produced by electromagnets.

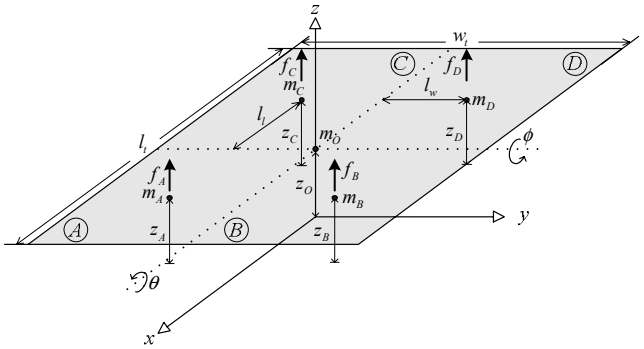

Fig. 2. Sketch diagram of maglev system.

According to Newtonian law and energy conservation principle, the dynamic model of the maglev system can be expressed as follows:

$$\mathbf{M}\ddot{\boldsymbol{x}}+\mathbf{B}\dot{\boldsymbol{x}}=\mathbf{G}_s\boldsymbol{u}_i-\boldsymbol{w}-\boldsymbol{d} \tag{1}$$

where $\boldsymbol{x}=[z_O \quad \theta \quad \phi \quad 0]^T$ is the system state vector; $\boldsymbol{u}_i=[i_A^2 \quad i_B^2 \quad i_C^2 \quad i_D^2]^T$ is the control current vector; $\mathbf{G}_s=\begin{bmatrix}1&1&1&1\\1&-1&1&-1\\1&1&-1&-1\\1&-1&-1&1\end{bmatrix}$ is an invertible constant matrix. Since the actual measurable variables are the central levitation heights of four sub-platforms, the relation of the

central levitation heights $\boldsymbol{z}=[z_A \quad z_B \quad z_C \quad z_D]^T$ and system states (z_O, θ, ϕ) can be transferred by

$$z_A = z_O - l_w \sin\theta - l_l \sin\phi, \quad z_B = z_O + l_w \sin\theta - l_l \sin\phi$$
$$z_C = z_O - l_w \sin\theta + l_l \sin\phi, \quad z_D = z_O + l_w \sin\theta + l_l \sin\phi \quad (2)$$

Suppose that **M**, **B**, $\boldsymbol{w}$, and $\boldsymbol{d}$ in (1) are nominal values of system parameter vectors and denote unknown actual values of **M**, **B**, $\boldsymbol{w}$, and $\boldsymbol{d}$ by $\bar{\mathbf{M}}$, $\bar{\mathbf{B}}$, $\bar{\boldsymbol{w}}$, and $\bar{\boldsymbol{d}}$, the actual dynamic model with an unknown external disturbance $\boldsymbol{f}_{d0}$ can be represented realistically as

$$\mathbf{M}\ddot{\boldsymbol{x}} + \mathbf{B}\dot{\boldsymbol{x}} + \boldsymbol{l}_u = \mathbf{G}_s \boldsymbol{u}_i - \boldsymbol{w} - \boldsymbol{d} \quad (3)$$

where $\boldsymbol{l}_u = \{\mathbf{M}\bar{\mathbf{M}}^{-1}(\bar{\mathbf{B}}\dot{\boldsymbol{x}} + \boldsymbol{f}_{d0} - \mathbf{G}_s \boldsymbol{u}_i + \bar{\boldsymbol{w}} + \bar{\boldsymbol{d}}) - (\mathbf{B}\dot{\boldsymbol{x}} - \mathbf{G}_s \boldsymbol{u}_i + \boldsymbol{w} + \boldsymbol{d})\}$ denotes the lumped uncertainty vector and its bound is assumed to be given by

$$\|\boldsymbol{l}_u\| < \rho \quad (4)$$

in which $\|\cdot\|$ is the Euclidean norm, and ρ is a given positive constant.

III. Backstepping-based Control Systems

In this section, the proposed backstepping control (BSC) scheme for the maglev system is described. The control problem is to find a suitable control law so that the system states can track desired reference commands. To achieve this control objective, define an error state vector $\boldsymbol{e} = \boldsymbol{x} - \boldsymbol{x}_d$ and its derivative $\dot{\boldsymbol{e}} = \dot{\boldsymbol{x}} - \dot{\boldsymbol{x}}_d$. Reformulate (3) via $\boldsymbol{u}_c^v = \mathbf{G}_s \boldsymbol{u}_i - \boldsymbol{w}$ as

$$\ddot{\boldsymbol{x}} = -\mathbf{M}^{-1}\mathbf{B}\,\dot{\boldsymbol{x}} - \mathbf{M}^{-1}\boldsymbol{d} - \mathbf{M}^{-1}\boldsymbol{l}_u + \mathbf{M}^{-1}\boldsymbol{u}_c^v \quad (5)$$

By viewing $\dot{\boldsymbol{x}}$ as a virtual control input (i.e., $\boldsymbol{\alpha}_1 \equiv \dot{\boldsymbol{x}}$ is chosen as the control input for the $\boldsymbol{e}$-subsystem) and considering a first Lyapunov function candidate $V_1 = \boldsymbol{e}^T\boldsymbol{e}/2$, whose derivative is $\dot{V}_1 = \boldsymbol{e}^T\dot{\boldsymbol{e}} = \boldsymbol{e}^T(\boldsymbol{\alpha}_1 - \dot{\boldsymbol{x}}_d)$, then there exists a stabilizing controller $\boldsymbol{\alpha}_1 = -\mathbf{K}_1\boldsymbol{e} + \dot{\boldsymbol{x}}_d$ such that $\dot{V}_1 = -\boldsymbol{e}^T\mathbf{K}_1\boldsymbol{e} \le 0$, in which $\mathbf{K}_1$ is a diagonal positive-definite matrix. Since the derivative of V_1 is a negative-definite function, it can imply that the error state vector $\boldsymbol{e} = 0$ is asymptotically stable.

In order to design an actual control effort for ensuring the stability of the maglev system in (5), a virtual error vector is defined as $\boldsymbol{e}_s = \dot{\boldsymbol{x}} - \boldsymbol{\alpha}_1$ and its derivative can be represented by

$$\dot{\boldsymbol{e}}_s = \ddot{\boldsymbol{x}} - \dot{\boldsymbol{\alpha}}_1 = -\mathbf{M}^{-1}\mathbf{B}\,\dot{\boldsymbol{x}} - \mathbf{M}^{-1}\boldsymbol{d} - \mathbf{M}^{-1}\boldsymbol{l}_u + \mathbf{M}^{-1}\boldsymbol{u}_c^v - \dot{\boldsymbol{\alpha}}_1 \quad (6)$$

Consider a second Lyapunov function candidate $V_2 = V_1 + \boldsymbol{e}_s^T\mathbf{K}_s\mathbf{M}\boldsymbol{e}_s/2$ with a diagonal positive-definite matrix $\mathbf{K}_s$ and take the derivative of V_2 with respect to time, there exists a BSC law as follows such that $\dot{V}_2 \le -\boldsymbol{e}^T\mathbf{K}_1\boldsymbol{e} - \boldsymbol{e}_s^T\mathbf{K}_s\boldsymbol{e}_s \le 0$.

$$\boldsymbol{u}_{c,BSC}^v = \mathbf{B}\dot{\boldsymbol{x}} + \boldsymbol{d} + \mathbf{M}\dot{\boldsymbol{\alpha}}_1 - 0.5\dot{\mathbf{M}}\boldsymbol{e}_s - \boldsymbol{e}_s - \mathbf{K}_s^{-1}\boldsymbol{e} - \rho\,\mathrm{sgn}[(\boldsymbol{e}_s^T\mathbf{K}_s)^T] \quad (7)$$

where $\mathrm{sgn}[\cdot]$ is a sign function vector. Since the derivative of V_2 is a negative-definite function, it can imply that the state vectors $\boldsymbol{e}$ and $\boldsymbol{e}_s$ go to zero asymptotically. According to Lyapunov theorem [19], [20], the stability of the BSC system can be guaranteed with $\|\boldsymbol{l}_u\| < \rho$. According to (7) and $\boldsymbol{u}_c^v = \mathbf{G}_s\boldsymbol{u}_i - \boldsymbol{w}$, the control current vector to electromagnets can be obtained as

$$\boldsymbol{u}_{i,BSC} = \mathbf{G}_s^{-1}(\boldsymbol{u}_{c,BSC}^v + \boldsymbol{w}) \quad (8)$$

However, the parameter variations of the system are difficult to measure, and the exact values of the external disturbance and unmodeled dynamics are also difficult to know in advance for practical applications. Selection of the upper bound of the lumped uncertainty vector has a significant effect on the control performance. If the uncertainty bound is selected too large, the sign function in (7) will result in serious chattering phenomena in the control efforts. The undesired chattering control efforts will wear the mechanical structure and might excite unstable system dynamics. On the other hand, if the uncertainty bound is selected too small, the stability conditions may be not satisfied. It will cause the controlled system to be unstable. In addition, the control currents belong to nonnegative inputs in the EMS system. To deal with the problem of nonnegative control inputs, the BSC law in (7) has to be transformed to actual control currents according to (8). To ensure the stability of the controlled system despite the existence of the uncertainties, alleviate chattering phenomena in control efforts, and avoid redundant transformation steps, a robust fuzzy-neural-network control (RFNNC) system is introduced in the following section.

IV. Robust Fuzzy-Neural-Network Control

In order to control the states of the maglev system more effectively, a robust fuzzy-neural-network control (RFNNC) system as shown in Fig. 3 is constructed in this section.

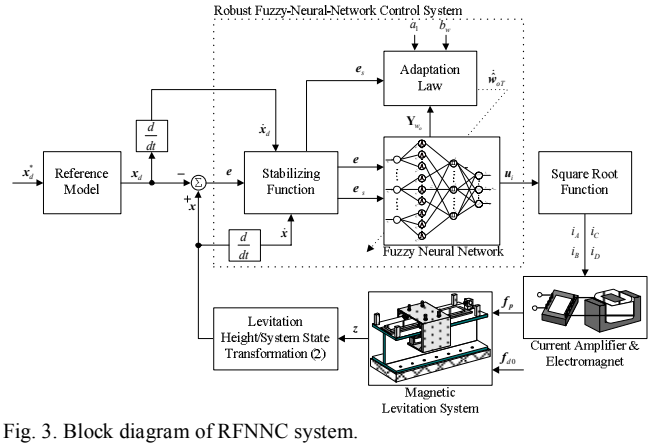

Fig. 3. Block diagram of RFNNC system.

Moreover, a four-layer fuzzy neural network (FNN), which comprises the input, membership, rule and output layers, is adopted to implement the RFNNC system in this study [16].

The inputs of the FNN are the elements in the error function vector defined as $\boldsymbol{q}=[e_1 \quad e_2 \quad e_3 \quad e_{s1} \quad e_{s2} \quad e_{s3}]$, in which (e_1, e_2, e_3) and (e_{s1}, e_{s2}, e_{s3}) are the elements in the error state vector $(\boldsymbol{e})$ and virtual error vector $(\boldsymbol{e}_s)$ relative to central levitation height, rolling angle and pitching angle, respectively. In addition, the output of the FNN is the control current vector. The signal propagation and the basic function in each layer of the FNN are introduced in the following paragraph.

1) Input layer transmits the input linguistic variables $q_i \ (i=1,\cdots,n)$ to the next layer, where q_i denotes the elements in the error function vector, $\boldsymbol{q}$.

2) Membership layer represents the input values with the following Gaussian membership functions:

$$\mu_i^j(q_i)=\exp[-(q_i-m_i^j)^2/(c_i^j)^2] \tag{9}$$

where $\exp(\cdot)$ is an exponential operator; m_i^j and $c_i^j \ (i=1,\cdots,n; j=1,\cdots,N_{p_i})$, respectively, are the mean and standard deviation of the Gaussian function in the *j*th term of the *i*th input linguistic variable q_i to the node of this layer. In order to represent the general case including different clusters with respect to the network inputs, the symbol N_{p_i} is utilized to denote the individual number of membership functions. For ease of notation, define parameter vectors $\boldsymbol{m}$ and $\boldsymbol{c}$ collecting all mean and standard deviation of Gaussian membership functions as $\boldsymbol{m}=[m_1^1 \cdots m_1^{N_{p1}} \ m_2^1 \cdots m_2^{N_{p2}} \cdots m_n^1 \cdots m_n^{N_{pn}}]^T \in R^{N_r\times 1}$ and $\boldsymbol{c}=[c_1^1 \cdots c_1^{N_{p1}} \ c_2^1 \cdots c_2^{N_{p2}} \cdots c_n^1 \cdots c_n^{N_{pn}}]^T \in R^{N_r\times 1}$, where $N_r=\sum_{i=1}^{n} N_{p_i}$ denotes the total number of membership functions.

3) Rule layer implements the fuzzy inference mechanism, and each node in this layer multiplies the input signals and outputs the result of the product. The output of this layer is given as

$$l_k=\prod_{i=1}^{n} w_{ji}^k \, \mu_i^j(q_i) \tag{10}$$

where $l_k \ (k=1,\cdots,N_y)$ represents the *k*th output of the rule layer and all values can be collected by a parameter vector $\boldsymbol{l}=[l_1 \quad l_2 \quad \cdots \quad l_{N_y}]^T$; w_{ji}^k, the weights between the membership layer and the rule layer, are assumed to be unity; N_y is the total number of rules.

4) Layer four is the output layer, and nodes in this layer represent output linguistic variables. Each node $y_o \ (o=1,\cdots,N_o)$ computes the output as the summation of all input signals with the following type:

$$y_o=f_o\Big(\sum_{k=1}^{N_y} w_k^o l_k\Big)=\sigma/[1+\exp(-\sum_{k=1}^{N_y} w_k^o l_k)] \tag{11}$$

where $f_o(\cdot)$ is the sigmoid activation function; σ is a positive constant; w_k^o, the adjustable weights between the rule layer and the output layer, can be gathered by the following matrix:

$$\mathbf{W}=[\boldsymbol{w}_{o1} \quad \boldsymbol{w}_{o2} \quad \cdots \quad \boldsymbol{w}_{oN_o}]^T \tag{12}$$

in which $\boldsymbol{w}_{oi}=[w_1^i \quad w_2^i \quad \cdots \quad w_{N_y}^i]$. Moreover, the output of the FNN can be rewritten in the following vector form:

$$\boldsymbol{y}=[y_1 \quad y_2 \quad \cdots \quad y_{N_o}]^T \equiv \boldsymbol{u}_{FNN}(\boldsymbol{q},\mathbf{W},\boldsymbol{m},\boldsymbol{c}) \tag{13}$$

The proposed RFNNC scheme comprises a FNN control and its associated network parameters tuning algorithm. The FNN control is designed to mimic the BSC law in (8) to maintain the robust control performance without the requirement of system information and auxiliary compensated control. Moreover, the network parameters tuning laws are derived in the sense of projection algorithm [13] and Lyapunov stability theorem [19], [20] to ensure the network convergence as well as stable control performance. According to the powerful approximation ability [12], there exists an optimal FNN control $\boldsymbol{u}_{FNN}^*$ to learn the BSC law, $\boldsymbol{u}_{i,BSC}$, such that

$$\boldsymbol{u}_{i,BSC}=\boldsymbol{u}_{FNN}^*(\boldsymbol{q},\mathbf{W}^*,\boldsymbol{m},\boldsymbol{c})+\boldsymbol{\varepsilon} \tag{14}$$

where $\boldsymbol{\varepsilon}$ is a minimum reconstructed error vector; $\mathbf{W}^*$ is the optimal parameter of $\mathbf{W}$ in the FNN. Design the control current vector as

$$\boldsymbol{u}_i=\hat{\boldsymbol{u}}_{FNN}(\boldsymbol{q},\hat{\mathbf{W}},\boldsymbol{m},\boldsymbol{c}) \tag{15}$$

where $\hat{\mathbf{W}}$ is the estimate of $\mathbf{W}^*$, as provided by tuning algorithm to be introduced later. Subtracting (15) from (14), an approximation error $\tilde{\boldsymbol{u}}_i$ is defined as

$$\tilde{\boldsymbol{u}}_i=\boldsymbol{u}_{i,BSC}-\boldsymbol{u}_i=\boldsymbol{u}_{FNN}^*+\boldsymbol{\varepsilon}-\hat{\boldsymbol{u}}_{FNN} \tag{16}$$

The linearization technique is employed to transform the sigmoid activation functions into partially linear form so that the expansion of $\tilde{\boldsymbol{u}}_i$ in Taylor series to obtain

$$\begin{aligned}\tilde{\boldsymbol{u}}_i&=\begin{bmatrix} \partial y_1/\partial \boldsymbol{w}_{o1}\,|_{\boldsymbol{w}_{o1}=\hat{\boldsymbol{w}}_{o1}}\,(\boldsymbol{w}_{o1}^{*T}-\hat{\boldsymbol{w}}_{o1}^{T})+o_{nv1} \\ \partial y_2/\partial \boldsymbol{w}_{o2}\,|_{\boldsymbol{w}_{o2}=\hat{\boldsymbol{w}}_{o2}}\,(\boldsymbol{w}_{o2}^{*T}-\hat{\boldsymbol{w}}_{o2}^{T})+o_{nv2} \\ \vdots \\ \partial y_{N_o}/\partial \boldsymbol{w}_{oN_o}\,|_{\boldsymbol{w}_{oN_o}=\hat{\boldsymbol{w}}_{oN_o}}\,(\boldsymbol{w}_{oN_o}^{*T}-\hat{\boldsymbol{w}}_{oN_o}^{T})+o_{mvN_o} \end{bmatrix}+\boldsymbol{\varepsilon} \\ &=\mathbf{Y}_{w_o}\tilde{\boldsymbol{w}}_{oT}+\boldsymbol{y}'\end{aligned} \tag{17}$$

where $\tilde{\boldsymbol{w}}_{oi}=\boldsymbol{w}_{oi}^*-\hat{\boldsymbol{w}}_{oi}$; $\boldsymbol{w}_{oi}^*$ is the optimal parameter of $\boldsymbol{w}_{oi}$, $\tilde{\boldsymbol{w}}_{oi}\in R^{1\times N_y}$; $\hat{\boldsymbol{w}}_{oi}$ is the estimate of $\boldsymbol{w}_{oi}^*$; $\boldsymbol{o}_{nv}\in R^{N_o\times 1}$ is a vector of higher-order terms; $\mathbf{Y}_{w_o}=diag[\boldsymbol{y}_{w_{o1}} \quad \boldsymbol{y}_{w_{o2}} \quad \cdots \quad \boldsymbol{y}_{w_{oN_o}}]\in R^{N_o\times N_{oy}}$, in which $N_{oy}=N_o\times N_y$; $\tilde{\boldsymbol{w}}_{oT}=[\tilde{\boldsymbol{w}}_{o1}^T \quad \tilde{\boldsymbol{w}}_{o2}^T \quad \cdots \quad \tilde{\boldsymbol{w}}_{oN_o}^T]^T\in R^{N_{oy}\times 1}$; $\boldsymbol{y}'=\boldsymbol{\varepsilon}+\boldsymbol{o}_{mv}$.

Consider a maglev system including actuator dynamics represented by (5), if the RFNNC law is designed as (15) and the adaptation laws of the FNN parameters are designed as (18), then the convergence of network parameters and tracking error of the proposed RFNNC system can be

assured.

$$\dot{\hat{\boldsymbol{w}}}_{oT} = -a_1(\boldsymbol{e}_s^T \mathbf{K}_s \mathbf{G}_s \mathbf{Y}_{w_o})^T$$

If $(\|\hat{\boldsymbol{w}}_{oT}\| < b_w)$ or $(\|\hat{\boldsymbol{w}}_{oT}\| = b_w$ and $\boldsymbol{e}_s^T \mathbf{K}_s \mathbf{G}_s \mathbf{Y}_{w_o} \hat{\boldsymbol{w}}_{oT} \le 0)$ (18a)

$$\dot{\hat{\boldsymbol{w}}}_{oT} = -a_1(\boldsymbol{e}_s^T \mathbf{K}_s \mathbf{G}_s \mathbf{Y}_{w_o})^T - a_1[\boldsymbol{e}_s^T \mathbf{K}_s \mathbf{G}_s \mathbf{Y}_{w_o} (\hat{\boldsymbol{w}}_{oT} \hat{\boldsymbol{w}}_{oT}^T / \|\hat{\boldsymbol{w}}_{oT}\|^2)]^T$$

if $(\|\hat{\boldsymbol{w}}_{oT}\| = b_w$ and $\boldsymbol{e}_s^T \mathbf{K}_s \mathbf{G}_s \mathbf{Y}_{w_o} \hat{\boldsymbol{w}}_{oT} > 0)$ (18b)

where a_1 is a positive learning rate, and b_w is a given positive parameter bound.

V. Numerical Simulations

The detail parameters of the moving platform are listed as follows:

$$l_t = w_t = 134\,\text{mm},\ l_l = l_w = 33.5\,\text{mm},\ z_{O,\max} = 5\,\text{mm},$$
$$m_{m_A} = m_{m_B} = m_{m_C} = m_{m_D} = 3.65\,\text{kg} \quad (19)$$

Numerical simulations of the BSC and RFNNC systems are implemented via the MATLAB software. Moreover, a second-order transfer function of the following form with rise time 0.2s is chosen as the reference model, which is used to specify the reference trajectories for the position and angle of the moving platform, for step commands:

$$\frac{\omega_n^2}{s^2 + 2\zeta\omega_n s + \omega_n^2} = \frac{81}{s^2 + 18s + 81} \quad (20)$$

where s is the Laplace operator; ζ and ω_n are the damping ratio (set at one for critical damping) and undamped natural frequency. In addition, mean-square-error (MSE) measures of the position and angle responses are defined as

$$MSE(x_i) = \frac{1}{T}\sum_{r=1}^{T} e_i^2(r) \quad (21)$$

where x_i and e_i indicate the elements of the system state vector $\boldsymbol{x} = [z_O \quad \theta \quad \phi \quad 0]^T$ and the corresponding error state vector, $\boldsymbol{e}$; T is total sampling instants. According to (21), the normalized-mean-square-error (NMSE) values of the position response (the angle response) using per-unit values with a 10^{-6}-mm base (10^{-6}-degree base) are used for examining the control performance in this study.

To investigate the robustness of the proposed control systems, the following two cases with parameter variations and time-varying external disturbance are considered:

Case 1) Initial system state: $z_O(0) = 0.2\,\text{mm}$, $\theta(0) = 0^\circ$, $\phi(0) = 0^\circ$; Parameter variations: loading by a weight of 0.5kg on m_C at 3s and unloading at 8s; External disturbance: $\boldsymbol{f}_{d0} = [2\pi\sin(\pi t) \quad \sin(\pi t) \quad \cos(\pi t) \quad 0]^T$ occurring at 2s.

Case 2) Initial system state: $z_O(0) = 2.1\,\text{mm}$, $\theta(0) = 1^\circ$, $\phi(0) = -0.8^\circ$; Parameter variations: loading by a weight of 1.0kg on m_O at 3s and unloading at 8s; External disturbance: $\boldsymbol{f}_{d0} = [2\pi\sin(\pi t) \quad \sin(\pi t) \quad \cos(\pi t) \quad 0]^T$ occurring at 2s.

Moreover, the control parameters of the BSC and RFNNC systems are given as follows:

$$\mathbf{K}_1 = diag(500,150,150,150),\ \mathbf{K}_s = diag(7,5,5,5),$$
$$\sigma = 225,\ a_1 = 1\times10^{-6},\ b_w = 8 \quad (22)$$

These parameters are chosen to achieve the best transient control performance in numerical simulations by considering the requirement of stability and the possible operating conditions. In this study, the control objective is to make the central levitation height of the moving platform follow the reference trajectory, and keep the corresponding rolling and pitching angles horizontal under the possible occurrence of uncertainties.

To show the effectiveness of the RFNNC system, the FNN has 6, 18, 729 and 4 neurons at the input, membership, rule and output layer, respectively. It can be regarded that the associated fuzzy sets with Gaussian function for each input signal are divided into N (negative), Z (zero) and P (positive), and the number of rules with complete rule connection is 729. Moreover, some heuristics can be used to roughly initialize the parameters of the RFNNC system for practical applications; e.g., the means and the standard deviations of the Gaussian functions can be determined according to the maximum variation of elements in the error function vector, $\boldsymbol{q}$. The numerical simulations of the proposed RFNNC system at cases 1 and 2 are depicted in Figs. 4 and 5, respectively. As can be seen from Figs. 4(a)–(c) and 5(a)–(c), the error state vector converges quickly, and the robust control characteristics under the occurrence of varied reference trajectories, parameter variations and external disturbance can be clearly observed. Because all parameters in the RFNNC are roughly initialized, the tracking errors are gradually reduced through on-line training process whether system uncertainties exist or not.

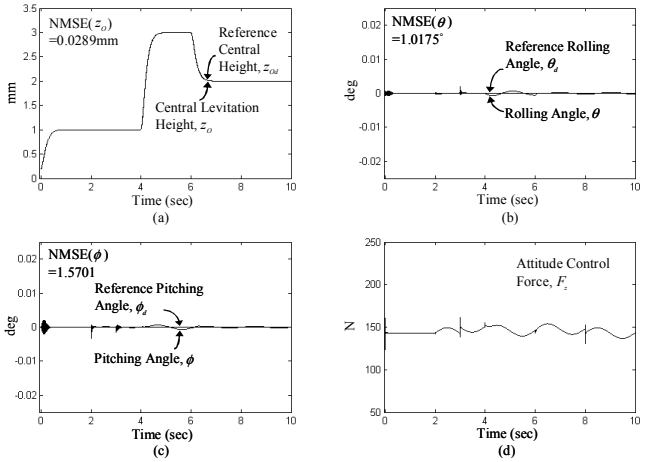

Fig. 4. Numerical simulations of RFNNC system at case 1: (a) Tracking response of central levitation height; (b) Rolling angle response; (c) Pitching angle response; (d) Attitude control force.

The performance comparisons of the BSC and RFNNC systems are summarized in Table I. According to the NMSE measures, the proposed RFNNC scheme has over 88.92%

height-tracking improvements and 67.40% angle-stabilizing improvements than the BSC system, respectively. From the comparison performed, it is clear that the proposed approach is more effective and efficient (no chattering) in performing levitation control than its BSC counterpart.

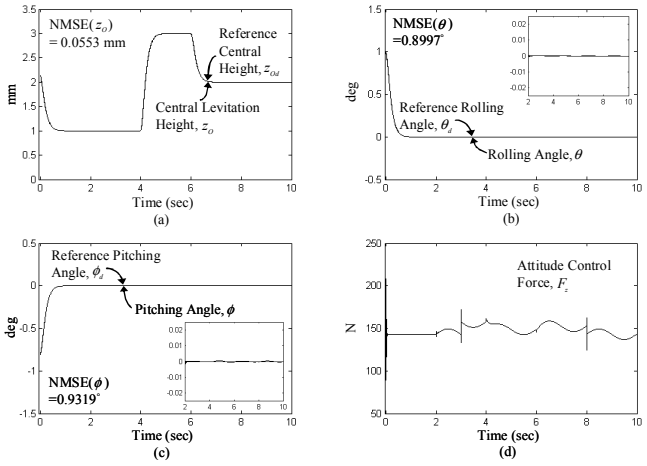

Fig. 5. Numerical simulations of RFNNC system at case 2: (a) Tracking response of central levitation height; (b) Rolling angle response; (c) Pitching angle response; (d) Attitude control force.

TABLE I

PERFORMANCE COMPARISONS OF BSC AND RFNNC SYSTEMS

Control Systems / Performance	BSC with $\rho = 1$		BSC with $\rho = 25$		RFNNC	
	Case 1	Case 2	Case 1	Case 2	Case 1	Case 2
NMSE(z_O)	176.1830mm	925.2410mm	0.3079mm	0.4993mm	0.0289mm	0.0553mm
NMSE(θ)	4.7318°	3.9161°	8.1511°	6.8327°	1.0175°	0.8997°
NMSE(ϕ)	4.8156°	3.4667°	8.0404°	6.8092°	1.5701°	0.9319°
Robustness	Poor		Fair		Favorable	
Chattering Phenomena	Small		Serious		None	
Dependence on System Parameters	High		High		Low	
Learning Ability	None		None		On-Line Learning	

VI. CONCLUSIONS

This study has successfully investigated the BSC and RFNNC systems for the levitation control of a linear maglev rail system. The RFNNC system has the salient merits of model-free control design, favorable robust characteristic, and control effort without chattering in comparison with the BSC systems. Thus, the proposed RFNNC system is more suitable for the levitation control of the linear maglev rail system than the BSC system. The major contributions of this study are the successful development of a model-free RFNNC methodology without the requirement of auxiliary compensated controllers, strict constrains and control transformations.

ACKNOWLEDGMENTS

The authors would like to acknowledge the financial support of the National Science Council of Taiwan, R.O.C. through grant number NSC 95-2221-E-155-085.

REFERENCES

[1] J. Kaloust, C. Ham, J. Siehling, E. Jongekryg, and Q. Han, "Nonlinear robust control design for levitation and propulsion of a maglev system," *IEE Proc. Contr. Theory Appl.,* vol. 151, no. 4, pp. 460–464, July 2004.

[2] P. Holmer, "Faster than a speeding bullet train," *IEEE Spectrum*, vol. 40, no. 8, pp. 30–34, Aug. 2003.

[3] C. T. Lin and C. P. Jou, "GA-based fuzzy reinforcement learning for control of a magnetic bearing system," *IEEE Trans. Syst., Man, Cybern., Part B,* vol. 30, no. 2, pp. 276–289, April 2000.

[4] O. S. Kim, S. H. Lee, and D. C. Han, "Positioning performance and straightness error compensation of the magnetic levitation stage supported by the linear magnetic bearing," *IEEE Trans. Ind. Electron.,* vol. 50, no. 2, pp. 374–378, April 2003.

[5] K. Nagaya and M. Ishikawa, "A noncontact permanent magnet levitation table with electromagnetic control and its vibration isolation method using direct disturbance cancellation combining optimal regulators," *IEEE Trans. Magn.,* vol. 31, no. 1, pp. 885–896, Jan. 1995.

[6] D. M. Tang, H. P. Gavin, and E. H. Dowell, "Study of airfoil gust response alleviation using an electro-magnetic dry friction damper. part 2: experiment," *Jour. Sound Vib.*, vol. 269, no. 3–5, pp. 875–897, Jan. 2004.

[7] W. J. Kim, D. L. Trumper, and J. H. Lang, "Modeling and vector control of planar magnetic levitator," *IEEE Trans. Ind. Appl.,* vol. 34, no. 6, pp. 1254–1262, Nov./Dec. 1998.

[8] M. Ono, S. Koga, and H. Ohtsuki, "Japan's superconducting maglev train," *IEEE Trans. Instrument. Meas. Mag.,* vol. 5, no. 1, pp. 9–15, March 2002.

[9] C. M. Huang, J. Y. Yen, and M. S. Chen, "Adaptive nonlinear control of repulsive maglev suspension systems," *Contr. Engin. Practice*, vol. 8, no. 12, pp.1357–1367, Dec. 2000.

[10] Y. He and F. L. Luo, "Sliding-mode control for dc–dc converters with constant switching frequency," *IEE Proc. Contr. Theory Appl.,* vol. 153, no. 1, pp. 37–45, Jan. 2006.

[11] J. Aracil, F. Gordillo, and E. Ponce, "Stabilization of oscillations through backstepping in high-dimensional systems," *IEEE Trans. Automat. Contr.,* vol. 50, no. 5, pp. 705–710, May 2005.

[12] C. T. Lin and C. S. George Lee, *Neural Fuzzy Systems*. NJ: Prentice-Hall, 1996.

[13] L. X. Wang, *A Course in Fuzzy Systems and Control*. NJ: Prentice-Hall, 1997.

[14] O. Omidvar and D. L. Elliott, *Neural Systems for Control*. Academic Press, 1997.

[15] D. Chakrborty and N. R. Pal, "Integrated feature analysis and fuzzy rule-based system identification in a neuro-fuzzy paradigm," *IEEE Trans. Syst., Man, Cybern., Part B,* vol. 31, no. 3, pp. 391–400, June 2001.

[16] F. J. Lin, W. J. Hwang, and R. J. Wai, "A supervisory fuzzy neural network control system for tracking periodic inputs," *IEEE Trans. Fuzzy Syst.*, vol. 7, no.1, pp. 41-52, Feb. 1999.

[17] Y. G. Leu, W. Y. Wang, and T. T. Lee, "Robust adaptive fuzzy-neural controllers for uncertain nonlinear systems," *IEEE Trans. Robot. Automat.*, vol. 15, no. 5, pp. 805-817, Oct. 1999.

[18] R. J. Wai and W. K. Liu, "Nonlinear control for linear induction motor servo drive," *IEEE Trans. Ind. Electron.*, vol. 50, no. 5, pp. 920–935, Oct. 2003.

[19] J.-J. E. Slotine and W. Li, *Applied Nonlinear Control*. Englewood Cliffs, NJ: Prentice-Hall, 1991.

[20] K. J. Astrom and B. Wittenmark, *Adaptive Control*. New York: Addison–Wesley, 1995.